LONGITUDINAL MOTION OF LOW-FLYING VEHICLES IN NONLINEAR FLOWFIELDS

ICAS-80-7.3

R.Staufenbiel and G. Kleineidam
Technical University of Aachen,
Aachen, F.R.G.

Abstract

Early in this century, it was discovered that a wing flying in close proximity to a surface experiences a reduction in induced drag. Performance and economic advantages have stimulated the concept of "wing-in-ground effect vehicles" (WIGs) intentionally operating within ground effect.

The paper is concerned with the strong interrelationship between aerodynamic configuration and longitudinal stability in ground effect. Airfoil characteristics and wing planforms have been analyzed under the aspect of static and dynamic height stability. Configurations suitable for the design of stable WIGs have been found.

By simulating flare maneuvers a comparison between a WIG and a conventional a/c has been made revealing the influence of aerodynamic configuration on longitudinal motion in ground effect.

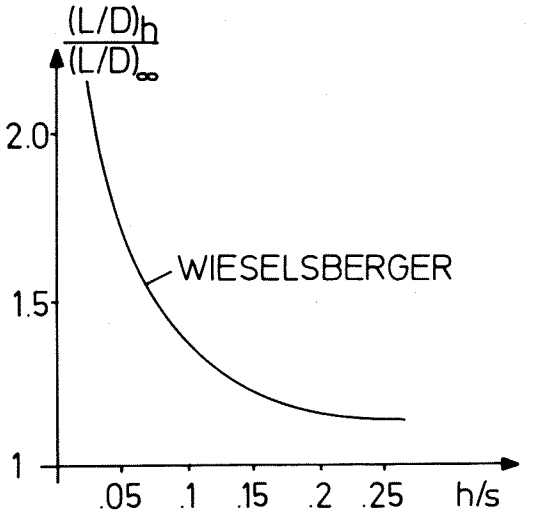

Fig. 1.1 Lift/drag ratio in ground effect

1. Introduction

It has been well known for many decades that a wing experiences a decrease in induced drag, if it is flown close to the ground. Fig. 1.1 gives the increase of lift/drag ratio for a wing with an elliptic lift distribution and is based on a theory developed by WIESELSBERGER (1), Professor at Aachen, 60 years ago.

The performance and economic advantages of vehicles flying just above the surface has stimulated the concept of "ram wing vehicles" or "wing-in-ground effect vehicles" (so called WIGs) intentionally operating within ground effect as some kind of fast travelling ships. Fig. 1.2 shows an experimental craft, built by Rhein-Flugzeugbau in Germany. This vehicle, the X-114, has been developed following a concept given by the late Alexander LIPPISCH (2).

Without going into details of future WIG configurations two basic ideas can be recognized:

1. Reduce the OWE by choosing a wing with low aspect ratio (AR = 2 - 3) and considering the low maneuver and gust loads in ground effect.

2. Increase the poor aerodynamic efficiency of the low AR wing by operating at very low heights.

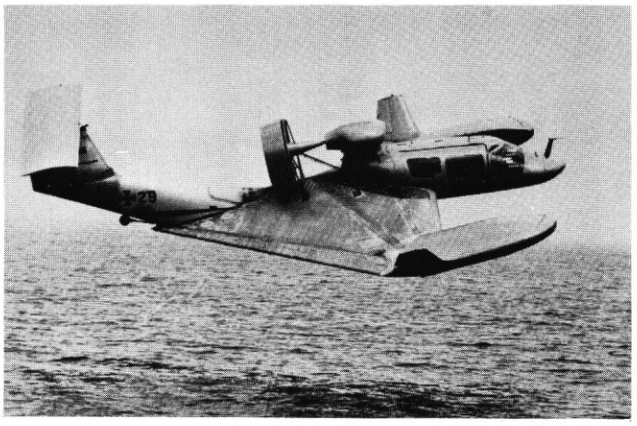

Fig. 1.2 Experimental WIG X-114 built by Rhein-Flugzeugbau in Germany

As Fig. 1.1 has shown, a reasonable increase of lift/drag ratio can only be gained, if the WIGs are operated at heights of about 10 % of the span. By fitting endplates or winglets to the wing a better lift/drag ratio can be achieved with higher ground clearance of the wing (3).

An interesting potential for generating additional wing lift is the power augmented ram-wing (PAR) proposed by GALLINGTON and KRAUSE (4). PAR might prove to be of great practical interest in water-based WIG design by providing means for avoiding high hydrodynamic drag during take-off.

Dealing with the design of WIGs a really unique problem has come up. A strong interrelationship between the aerodynamic shape of the vehicles and the dynamics of flight has been found as the typical and difficult problem of WIG design.

That was the reason why Alexander LIPPISCH had used a lot of free flying models to find a configuration which was dynamically stable i.g.e. The method of trial and error was finally successful due to the genius of LIPPISCH. What makes the problem worse in the fact that a theory of this interrelationship has to cope with nonlinear aerodynamics and flight mechanics.

2. Dynamics of Flight

2.1 Equations of Motion

At very low heights the aerodynamic coefficients in the longitudinal equations of motion, to which we are going to restrict ourselves, are essentially nonlinear functions of height h and angle of attack α . Therefore the concept of aerodynamic derivatives cannot strictly be applied because the derivatives can only be assumed constant for small perturbations. Nevertheless, for a general description of static and dynamic stability i.g.e. a quasilinear motion can be considered. The nonlinearity of the aerodynamic coefficients can be written approximately in the form:

$$C_D = f_D(\alpha, h/s) + C_{D_P} \tag{2.1a}$$

$$C_L = f_L(\alpha, h/\bar{c}) + C_{L\eta}\,\delta\eta \tag{2.1b}$$

$$C_m = f_m(\alpha, h/\bar{c}) + \frac{1}{\mu \hat{v}_0}\left[C_{mq}\frac{d\vartheta}{d\tau} + C_{m\dot{\alpha}}\, f_{m\dot{\alpha}}(h/\bar{c})\frac{d\alpha}{d\tau}\right] \tag{2.1c}$$

The longitudinal equations of motion are written in nondimensional units. Wind axes have been used as reference axes. The three equations can be written as

$$\frac{d\hat{v}}{d\tau} = \frac{T}{W} - C_D\hat{v}^2 - \sin\gamma \tag{2.2}$$

$$\hat{v}\frac{d\gamma}{d\tau} = C_L\hat{v}^2 - \cos\gamma \tag{2.3}$$

$$(2.4) \qquad \frac{d^2\vartheta}{d\tau^2} = \mu\left(\frac{\bar{c}}{i_y}\right)^2 C_m \hat{v}^2$$

We have also the kinematic relation

$$(2.5) \qquad \frac{d\hat{z}}{d\tau} = \hat{v}\sin\gamma$$

In the general case, Eqs. (2.1 - 2.5) have to be solved with given initial conditions and control inputs.

Linearization of the equations and the aerodynamic coefficients will be useful and acceptable if the effect of small disturbances on a rectilinear unaccelerated flight at constant height should be investigated.

Then, the essential influences of height and angle of attack on the aerodynamic coefficients Eqs.(2.1), using the concept of derivatives, can be written in the form

$$(2.6a) \qquad \delta c_D = c_{D\alpha}\,\delta\alpha + c_{Dh}\,\delta(h/\bar{c})$$

$$(2.6b) \qquad \delta c_L = c_{L\alpha}\,\delta\alpha + c_{Lh}\,\delta(h/\bar{c})$$

$$(2.6c) \qquad \delta c_m = c_{m\alpha}\,\delta\alpha + c_{mh}\,\delta(h/\bar{c}) + \frac{1}{\mu\hat{v}_0}\left[c_{m\dot{\alpha}}\frac{d\alpha}{d\tau} + c_{mq}\frac{d\vartheta}{d\tau}\right],$$

where fixed controls are assumed.

Linearization of the equations of motion and inserting Eqs. (2.6) gives a characteristic equation of the fifth order,

$$(2.7) \qquad s^5 + Bs^4 + Cs^3 + Ds^2 + Es + F = 0$$

which normally has two oscillatory modes and an aperiodic one.

The coefficients of the characteristic equation (2.7) depend on the derivatives in a very complicated manner. Therefore, it is difficult to get a basic understanding of the peculiarity of the motion in ground effect.

However, it seems to be possible to get a first insight into the problems involved, by considering the static stability.

2.2 Static Stability in Ground Effect

The criterion for static stability, in general sense, is the condition $F \gtrsim 0$. As shown in Ref. 5, the coefficient F can be factored into three parts:

$$(2.8) \qquad F \sim \left[-\frac{\partial c_m}{\partial\alpha}\right]_{\hat{v},h} \cdot \left[-\frac{\partial\left(\frac{T-D}{W}\right)}{\partial\hat{v}}\right]_{\substack{c_m=0 \\ n=1}} \cdot \left[-\frac{\partial n}{\partial(h/\bar{c})}\right]_{\hat{v},c_m=0}$$

The first factor is the "static pitching stability" well known as the "static stability" from analysis of flight under o.g.e. conditions.

The second term occurs in assessments of stability under constraints fixing the glide path angle and gives the "minimum drag speed" as the stability boundary.

The third factor is a new specific term containing just the most important influence of the ground effect. It gives a necessary condition for a stable flight at constant height near the ground. Therefore

$$(2.9) \qquad \left(\frac{\partial n}{\partial(h/\bar{c})}\right)_{\hat{v},c_m=0} < 0$$

is called the condition for "static height stability".

The physical interpretation of (2.9) is as simple as it is the case for the "static pitching stability". Whereas the first two terms in Eq. (2.8) provide statically stable equilibrium both at pitching and speed disturbances, the condition of Eq. (2.9) gives a restoring force, if the equilibrium in height is disturbed. First, let us consider a disturbance in height without any pitching motion (Fig. 2.1). Then the lift coefficient changing with height would give a restoring vertical force, if

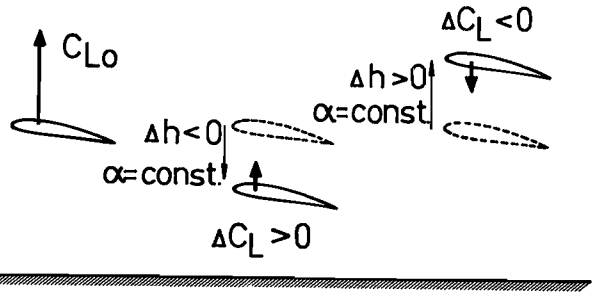

Fig. 2.1 The condition of height stability pitching neglected

$$(2.10) \qquad \frac{\Delta c_L}{\Delta h} < 0 \quad \text{or} \quad C_{Lh} < 0$$

In general, a vertical motion is coupled with a pitching motion (Fig. 2.2) which can be obtained by assuming equilibrium in pitch

$$\delta c_m = 0$$

$$\Delta\alpha = -\frac{c_{mh}}{c_{m\alpha}} \cdot \Delta(h/\bar{c})$$

Substituting $\Delta\alpha$ in Eq. (2.6b) leads to

$$\frac{\Delta c_L}{\Delta h/\bar{c}} = C_{Lh} - \frac{c_{mh}}{c_{m\alpha}} C_{L\alpha}$$

Equivalent to Eq. (2.10), the general conditions for static height stability are given by

$$(2.11) \qquad C_{Lh} < 0 \qquad \text{and}$$

$$F_m = \frac{c_{mh}}{(-c_{m\alpha})} \cdot \frac{c_{L\alpha}}{(-c_{Lh})} < 1$$

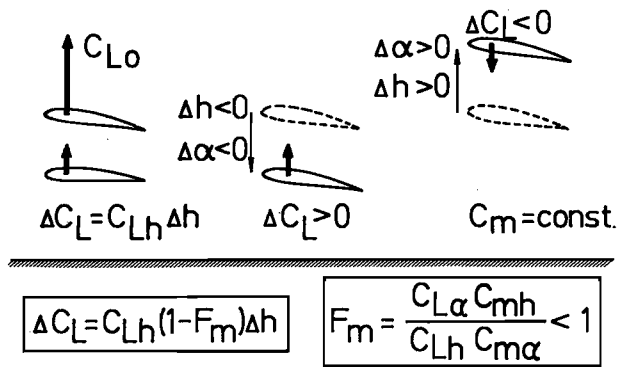

Fig. 2.2 General condition of static height stability

If a conventional wing with flaps deflected approaches the ground, there will be no static height stability because the lift decreases due to a reduction of the effective camber of the airfoil sections (Fig. 2.3) which is not compensated by the lift increase caused by the ram-effect. For wings with a smaller camber of the sections a negative c_{Lh} can be obtained. Then, in general, a nose-down pitching will result from the ram-effect on the lower side of the wing that is, $c_{mh} > 0$.

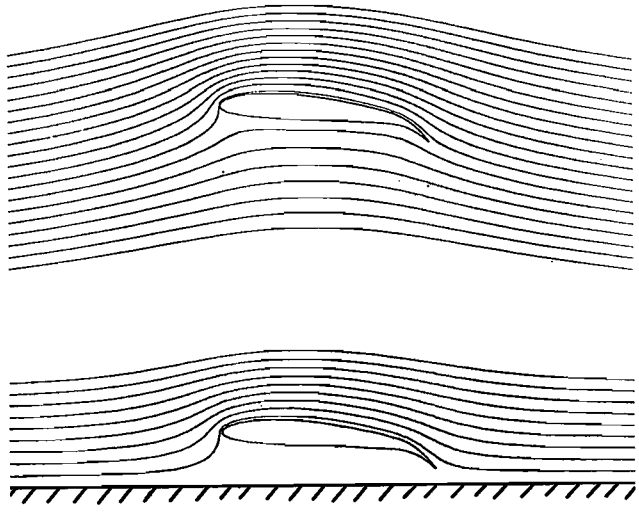

Fig. 2.3 Reduction of effective camber by ground effect

Therefore, to provide a ram-wing vehicle with a sufficient margin of static height stability, a high value of c_{mh} must be compensated by high values both of $(-c_{Lh})$ and static pitching stability $(-c_{m\alpha})$. The static pitching stability can be increased, without increasing c_{mh} as well, by a horizontal tail working out of ground effect. Such a configuration has been used very sucessfully for the X-113 and X-114.

2.3 Dynamic Stability in Ground Effect

The dynamic longitudinal stability of WIGs is determined by the roots of the fifth-order characteristic equation (2.7).

Going out of ground effect, the coefficient F in Eq. (2.7) disappears in the same way as the static height stability, a factor of F, is reduced. Then, it becomes the well-known quartic equation with the "short period mode" and the "phugoid mode" as solutions. Flying near the ground, an aperiodic mode is obtained in addition to a pair of complex roots. The root locus for a typical WIG configuration is given in Fig. 2.4 with height as a parameter.

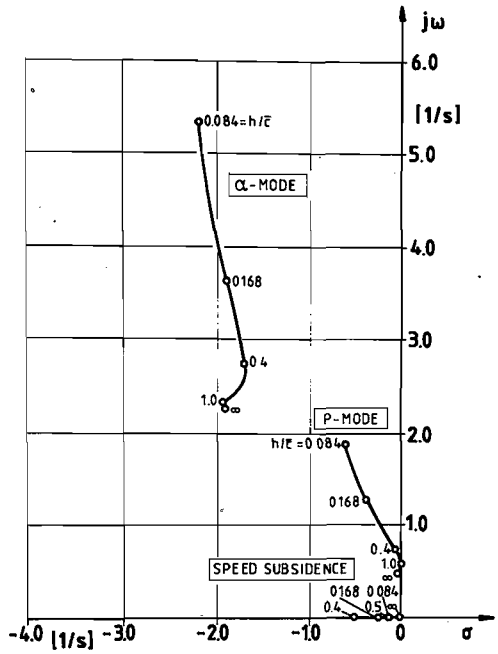

Fig. 2.4 Root loci of a typical WIG configuration

This root locus is valid for a vehicle of the X-113 or X-114 type. The main conclusions drawn from this diagram are the following.

(1) For a configuration of the X-113 type, dynamic stability is obtained in all modes if the vehicle flies near the ground ($h/\bar{c} \leq 0.5$)

(2) The root-locus branch which moves away from the short-period roots, the " α -branch", shows an increase in the natural frequency with a slight reduction of the damping ratio.

(3) The "P-branch", emanating from the low-frequency low-damping phugoid mode, indicates an increase in both natural frequency and damping ratio below $h/\bar{c} = 0.5$. The stability of the "P-branch" is equivalent to dynamic height stability. In a "transition phase" of heights ranging between $h/\bar{c} \approx 2$ and $h/\bar{c} = 0.5$ an unstable region is found. In this case artifical stabilization can be obtained by an airspeed-hold system.

(4) A time constant describes the transients following speed disturbances. The time constant is reduced, as a favourable effect, in the "transition phase" but increases again in flight at very low speed. The poor damping of speed disturbances is an influence of the reduction in induced drag.

3. The Influence of Airfoil Shapes on Height Stability

For the design of good ram-wing configurations it does not appear very useful to start with an investigation of airfoil characteristics. The influence of wing planform seems to be dominant, because wings with low aspect ratios (AR ≤ 3) will be favoured in ram-wing vehicles. However, it is just the gound effect which provides a nearly 2-dimensional flowfield at very low heights in the same way as it reduces the induced drag.

In the last decades work on airfoils in ground effect has covered only moderate heights ($h/\bar{c} \approx 1$) and aimed at the influence of the ground effect on maximum lift at take-off and landing of conventional aircraft (6). Very few papers have included low heights (7).

The strong interrelationship between aerodynamics and dynamics of flight, described in section 2, must very likely lead to the development of new airfoil shapes. The evaluation of existing profiles with regard to their possible use for WIGs will be started with the treatment of the basic aerodynamic and dynamic characteristics of the CLARK-Y profile, used in the prototypes X-113 and X-114. A 2-dimensional vortex method (8) (with a vortex distribution on the profile contours) was used to calculate pressure distribution, aerodynamic coefficient and c.p. as functions of height and angle of attack. In Fig. 3.1 the pressure coefficient is plotted for 4 different heights at a fixed angle of attack of 6°. It can be seen that the ground effect mainly influences the lower side of the airfoil. As the height decrease the pressure coefficient $c_p \rightarrow 1$ as an indication of the ram-effect. Fig. 3.2 gives the lift coefficient as a function of the angle of attack for four different heights. This diagram illustrates that in ground effect lift coefficient and lift curve slope increases with decreasing height only the former effect being favourable to static height stability.

Fig. 3.2 shows that all the plots of the lift coefficient meet nearly in one point at an angle of attack of -1°. In this point the lift coefficient is insensitive to changes in height and, therefore, height stability cannot obtained for lift coefficients near or below this point of intersection.

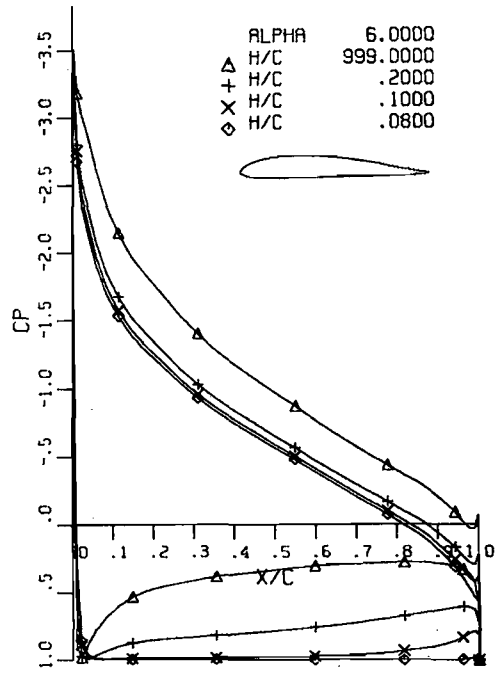

Fig. 3.1 Pressure distribution of a CLARK-Y airfoil

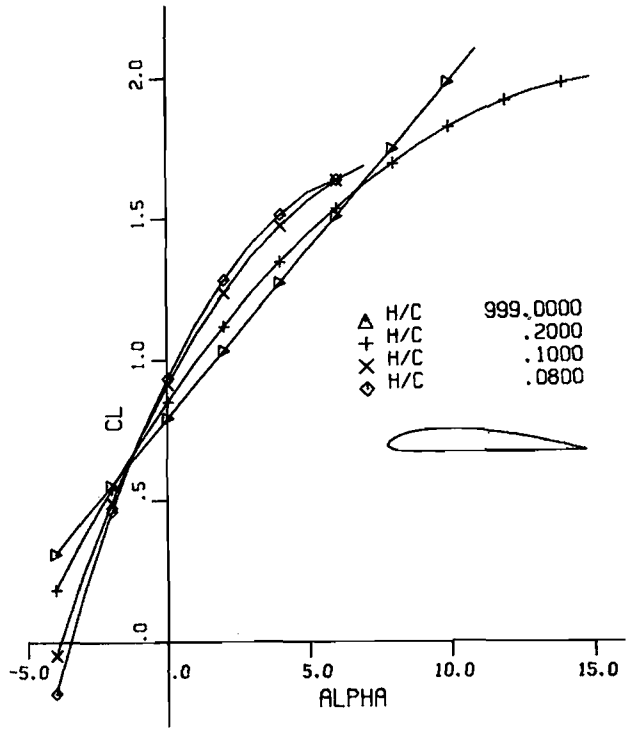

Fig. 3.2 Lift coefficient of a CLARK-Y airfoil

Below the point of intersection there is a loss of lift, compared with the out-of-ground condition, due to the fact that a suction force is built up at the lower side of the airfoil. (Fig. 3.3) For a comparison of different airfoil shapes the position of the point of intersection gives a rought indication of the stability characteristics.

The trouble with the condition of static height stability is that the stability parameter F_m connects all derivatives of lift and pitching moment with respect to height and angle of attack. Therefore it seems very difficult to find a real understanding of the relationship between airfoil shape and the stability parameter F_m.

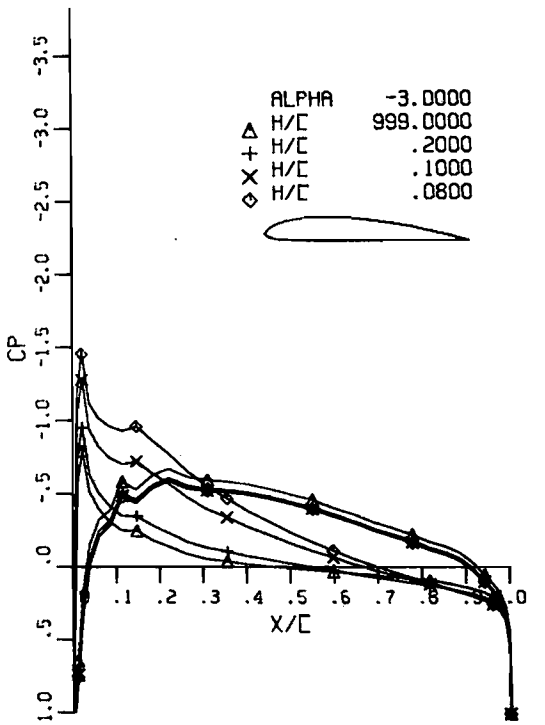

Fig. 3.3 Suction force near ground generating lift losses

The study of this problem will be much simplified, if we express the pitching moment derivatives in terms of the movement of c.p. position. If the c.p. of the airfoil had a fixed position in the whole regime of height and angle of attack, the airfoil would just be neutrally stable with respect to height disturbances as follows form

$$(3.1)\quad F_m = \frac{C_{mh}\cdot C_{L\alpha}}{C_{m\alpha}\cdot C_{Lh}} = \frac{(-x_p\cdot C_{Lh})\cdot C_{L\alpha}}{(-x_p\cdot C_{L\alpha})\cdot C_{Lh}} \equiv 1 .$$

x_p is the distance of the airfoil c.p. behind c.g. in units of the chord. In general, c.p. of an airfoil is not fixed but moves with changes in angle of attack and height. Therefore, the relation (3.1) must be modified. Inserting the movement of c.p. in the form of partial derivatives with respect to α and h leads to the following expression for the stability parameter F_m

$$(3.2)\quad F_m = \frac{x_p + (-x_{ph})\,C_L/(-C_{Lh})}{x_p - (-x_{p\alpha})\,C_L/C_{L\alpha}} .$$

Considering a CLARK-Y profile, the c.p. is shifted backwards with decreasing values of height and angle of attack, which leads to positive signs for all terms in brackets in Eq. (3.2). This implies that the CLARK-Y airfoil is inherently unstable in height. In this case height stability can only be accomplished by adding a horizontal tail which is kept out of ground*. Such a location was also used in the prototypes X-113 and X-114. It moves the c.p. rearwards with increasing α ($x_{p\alpha} > 0$) and leads to a favourable increase of the denominator in (3.2) without touching the numerator. Indeed, it is desirable to limit the horizontal tail volume as far as possible.

Let us now turn to the important subject of the influence of c.g. position on height stability. An examination of Eq. (3.2) leads to the following condition for height stability

$$(3.3)\quad (-x_{ph}) < \frac{(-C_{Lh})}{C_{L\alpha}}\cdot x_{p\alpha} .$$

*A canard would lead to a reduction of height stability.

Eq. (3.2) and (3.3) reveal two, perhaps surprising results

(1) The condition for height stability does not depend on the position of c.g. (expressed by x_p). Stability is only a matter of the aerodynamic configuration.

(2) For a basically stable configuration the stability margin, given by $(1-F_m)$, can be increased, if the c.g. is moved rearwards.

If a CLARK-Y profile is incorporated into a ram-wing configuration it can hardly be claimed as an airfoil very suitable to application in wing-in-ground vehicles due to the lack of height stability inherent in this profile. It would be highly desirable to find an airfoil shape and a wing planform which satisfies the condition of static height stability without requiring a horizontal tail. (A tail volume ratio of 0.6 was necessary to provide sufficient height stability of the X-114. This value is remarkably high considering the large wing volume of such vehicles). It is Eq. (3.3) which leads to the basic ideas for the design of a suitable airfoil.

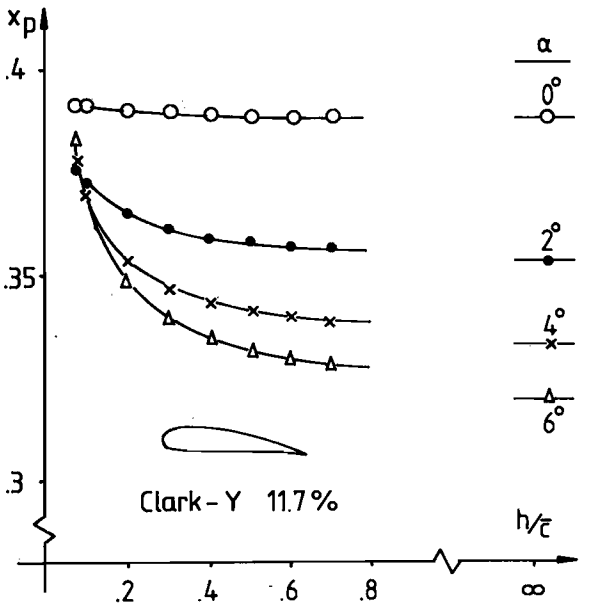

Fig. 3.4 Movement of c.p. with height and angle of attack

Height stability - equivalent to $(F_m < 1)$ - is favourably influenced by positive values of the derivatives of the c.p. position with respect to α and h. ($x_{p\alpha} > 0$ and $x_{ph} > 0$). If one of these derivatives is negative, the other one must be positive with a sufficiently high value. As a result of a parametric study, we found that in most cases the c.p. moves rearwards with decreasing values of height and angle of attack. This characteristic is just unfavourable with regard to height stability. The adverse effect of height is caused by the fact that the pressure distribution is getting more uniform at the lower side of the airfoil if it approaches the ground (ram-effect). The backward movement of c.p. with decreasing α results mainly from the negative zero-lift-pitching moment due to the positive camber of most of the conventional airfoils. The CLARK-Y profile belongs as well to this class (Fig. 3.4).

It was an important result that the ground effect mainly influences the pressure distribution at the lower side of an airfoil. Therefore the derivative of the c.p. position with height might be influenced mainly by choosing a suitable shape of the lower surface. We can expect that unloading the rear part of the lower surface which increases with ground proximity would be favourable to height stability.

It was this consideration which led to a simple way of augmenting height stability of the CLARK-Y profile. A trailing edge flap, deflected to an upward position, would unload the rear part of the airfoil. This effect is enlarged with decreasing height as can be seen in Fig. 3.5, where the pressure distribution of a CLARK-Y profile with a plain flap of chord ratio 0.1, deflected 6° upward, is presented at 4 different heights.

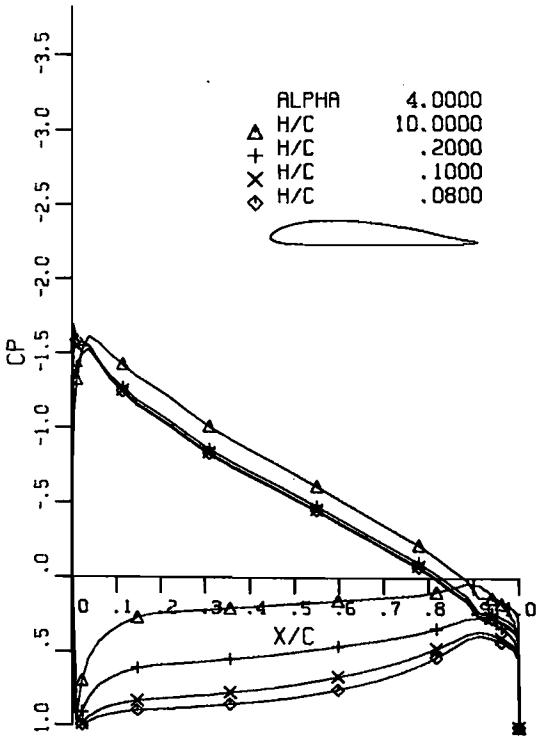

Fig. 3.5 Pressure distribution of a CLARK-Y airfoil with an upward deflected flap (η = -6°)

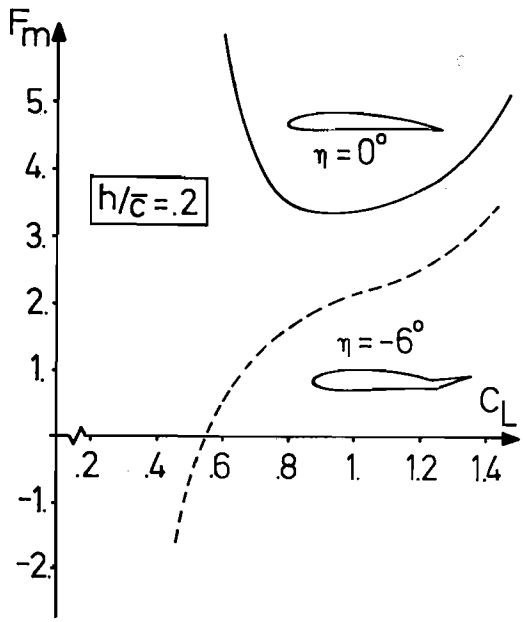

Fig. 3.6 Influence of the upward deflected flap on static height stability

This simple modification of the airfoil shape leads to a remarkable reduction of F_m (Fig. 3.6) which is favourable for static stability. Even a stable airfoil can be achieved at lower values of the lift coefficient $c_L < 0.8$.

It should be recognized that unloading the rear part of the airfoil mainly influences the derivative of the c.p. position with respect to height. The derivative of c.p. with respect to α will be favourable affected by decambering the airfoil.

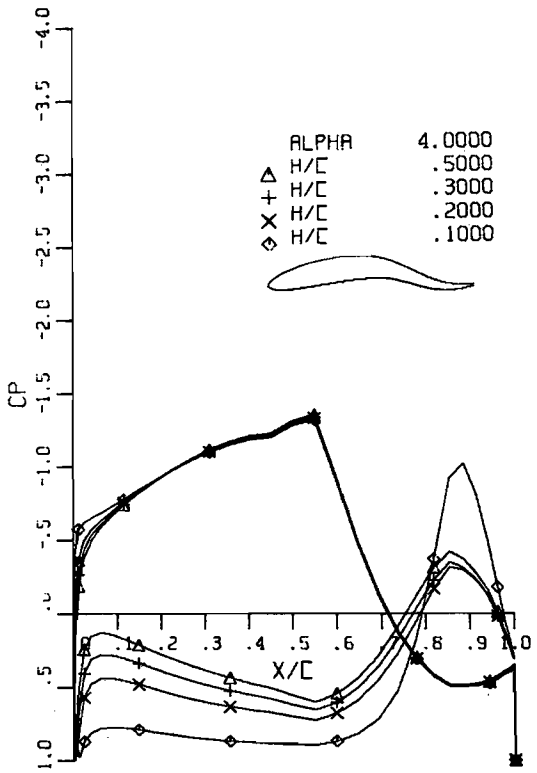

Fig. 3.7 Pressure distribution of an optimized airfoil for constant angle of attack

An example for such an airfoil is given in Fig. 3.7 It consists of an S-type shape. The pressure distribution for different heights and angles of attack can be seen in Fig. 3.7 and 3.8.

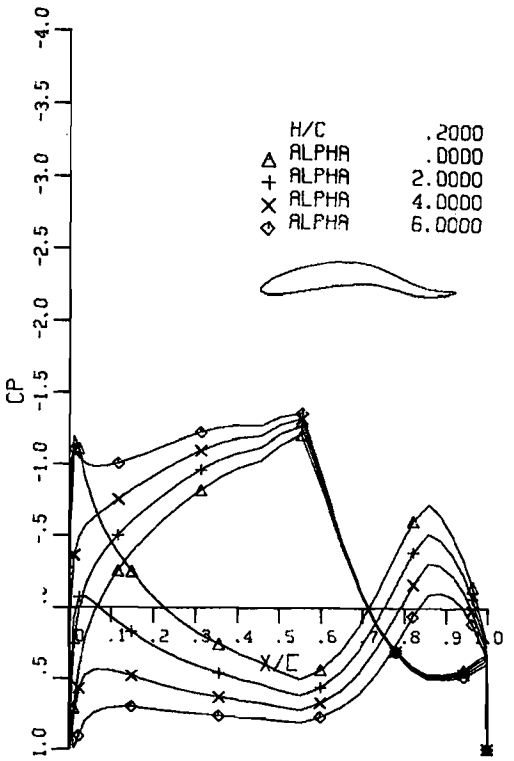

Fig. 3.8 Pressure distribution of an optimized airfoil (h = const)

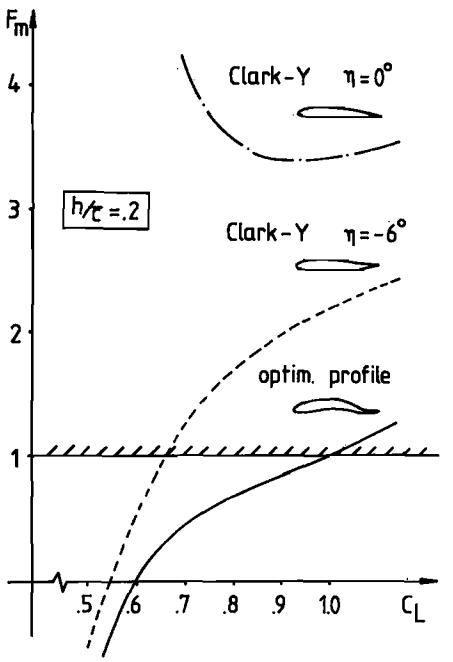

Fig. 3.9 Comparison of static height stability for three airfoils

The upper-surface pressure distribution is now practically independent of height. The distribution approaches a flat rooftop for higher angles of attack. The loading of this airfoil has a maximum in the middle part, while the loading is reduced at the leading edge and, obviously, much more at the trailing edge. A consequence of this distribution is that the c.p. will not move rearwards any longer, at least for moderate values of the lift coefficient. The favourable effect can be seen in Fig. 3.9 where the parameter of static height stability is plotted for the three types of airfoils presented so far. The shape of the airfoil last mentioned is the result of an optimization procedure. The mean line of the airfoil was approximated by a cubic spline function, the parameters of which have be varried in order to find a maximum range of lift coefficient where static height stability is obtained. The distribution of thickness was that of a 4-digit NACA profile, with 12 % thickness.

This section has reviewed some basic characteristics of airfoils in ground effect and has pointed out that the design of a suitable airfoil shape has to consider the strong interference between the aerodynamics and the flight dynamics. Static height stability, which is a necessary condition for safe flights near ground, cannot be obtained by shifting the c.g. into a suitable range. A horizontal tail of sufficient size would provide height stability but leads to a remarkable increase in structural weight. A stabilizing effect can be achieved by a suitable shaping of the airfoil section. Conventional airfoils are inherently unstable and require a very large stabilizing tail. Unloading the rear part of airfoil by deflecting plain flaps or using S-type shapes, combined with a reduction of the camber, shifts the c.p. position at changes in height and angle of attack in a stabilizing sense.

It is obvious that control actions which change

the effective airfoil shape, e.g. by deflecting control surfaces or flaps, have a direct strong impact on height stability, a fact which makes design even more difficult. Another important aspect must be left out. At a given low height, the ground clearance of the trailing edge or the point of maximum negative camber limits the highest usable lift coefficient. The corresponding angle of attack is, at low heights, far from the value for maximum lift out-of-ground. This effect should lead to a new type of high-lift systems.

This subject field, where a lot is to be done, should be left now with the remark that these results are not only important for designing ram-wing vehicles but could help to study the flight dynamics of conventional a/c in the last phase of landing.

4. Wing characteristics

In this section we will turn to the aerodynamics and flight dynamics of finite wings in ground effect.

The characteristics of airfoils are now mixed with an effect, peculiar to the finite wing. Replacing the ground plane by a mirror image of the wing, it is apparent that the mirror system of the trailing vortices induces an upwash on the wing which increases the effective incidence and reduces the induced drag. The reduction of the net downwash causes an increase in lift curve slope as height is reduced (Fig. 4.1).

However, the lift-curve slope of a finite wing must be smaller than the value of an airfoil inasmuch as there is no downwash at all on an airfoil. Consequences of this are

- a reduction of the maximum usable lift coefficient at a desired ground clearance of the trailing edge of the wing
- the point of intersection of the lift curves for different heights is shifted to a lower lift coefficient.

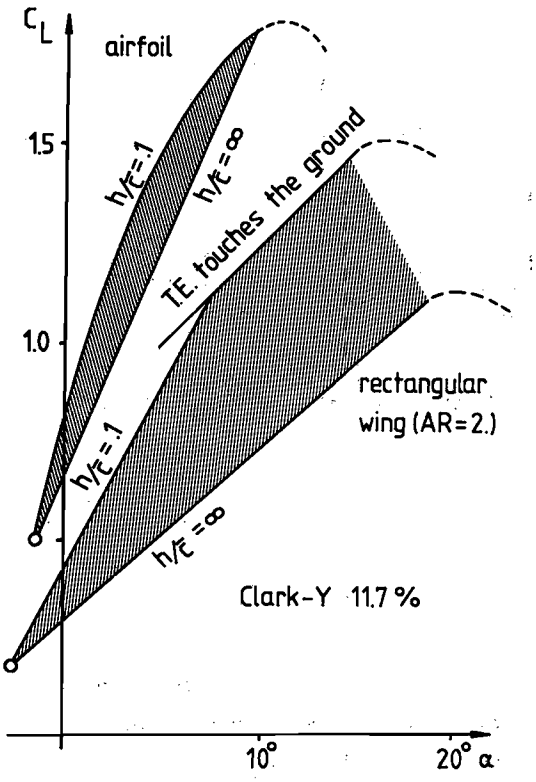

Fig. 4.1 Comparison between 2D/3D lift coefficients i.g.e.

The latter results is due to the fact that the lift coefficient of finite wings increases as height is reduced by an additional effect. A higher lift is obtained not only by means of the ram effect but also by an increase of the effective incidence due to the reduction of the downwash on finite wings approaching the ground. It is, of course, a desired effect inasmuch as the maximum speed,usable by ram-wing vehicles, is shifted to remarkably higher values.

The flowfield around finite wings is three-dimensional even in close proximity to the ground. This is illustrated by Fig. 4.2 where the pressure distribution of a rectangular wing with CLARK-Y sections is presented for three locations in spanwise direction. It might be surprising that ground effect is for finite wings still more a matter of the lower side of the surface than it was found for airfoils.

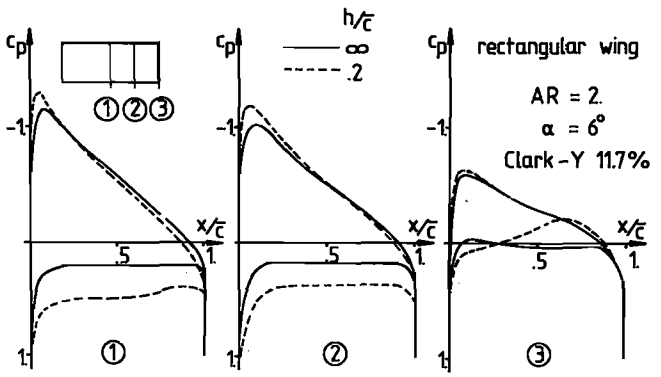

Fig. 4.2 Pressure distribution of a rectangular wing with CLARK-Y sections

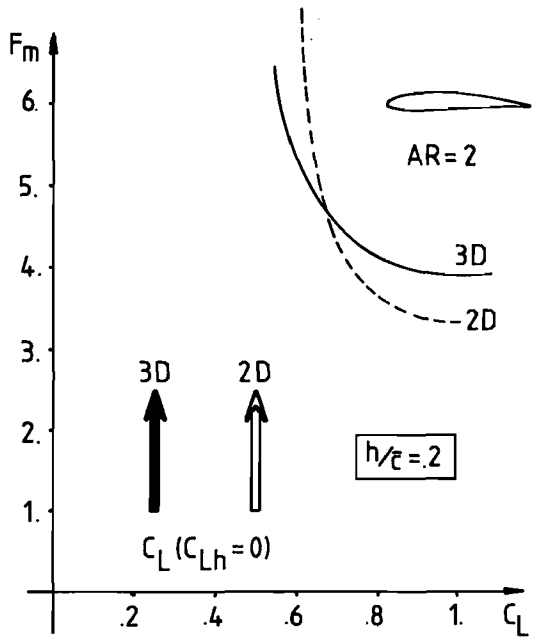

Fig. 4.3 Comparison of static height stability at 2D/3D flowfield

The pressure distribution of the inner sections of the wing corresponds to that of the airfoil, if we introduce effective incidence corrected by the induced angle of attack. It will be noted that only the pressure distribution near the wing tip is of different nature. It can be seen in Fig. 4.2 that an unloading of the rear part of the tip section takes place. The reason for this effect is the outflow in lateral direction, which gives a pressure drop near the T. E.of the wing tip.

Turning now to the problem of the static height stability, Fig. 4.3 illustrates that the stability parameter F_m does not show an essential difference between the airfoil and the wing characteristics.

The lower lift coefficient, found at the point of intersection of the lift curves ($c_{Lh} = 0$), results in a shifting of the singularity of the F_m-curve to this lower value of the lift coefficient. Refering to the pressure distribution in the inner section, one might suppose that the way of shaping the airfoil for better height stability, explained in the preceeding section, would also give better stability for a rectangular wing with the modified airfoil section. Choosing the flapped CLARK-Y as airfoil section, the effect upon F_m can be seen in Fig. 4.4. We may conclude, therefore, that incorporating an airfoil with better height stability

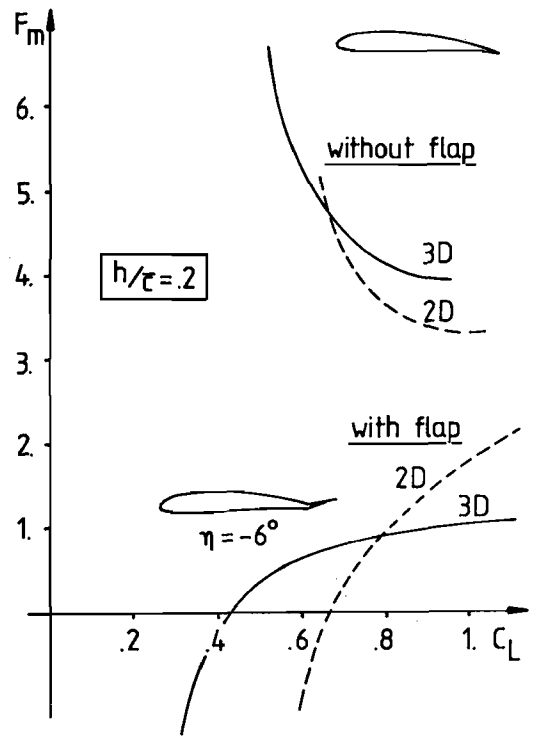

Fig. 4.4 Influence of flap deflection on static height stability (comparison 2D/3D)

would also make a ram-wing more stable. So far we have been only considering the inner sections of a rectangular wing. We are now going to turn to the wing tip section. The flow pattern near the wing tip can be modified by using endplates. By fitting suitable endplates at the wing tips the induced drag will be reduced, an effect which is well known for many decades. It is obvious that endplates will also modify the pressure distribution especially near the wing tips and could, therefore, influence the height stability.

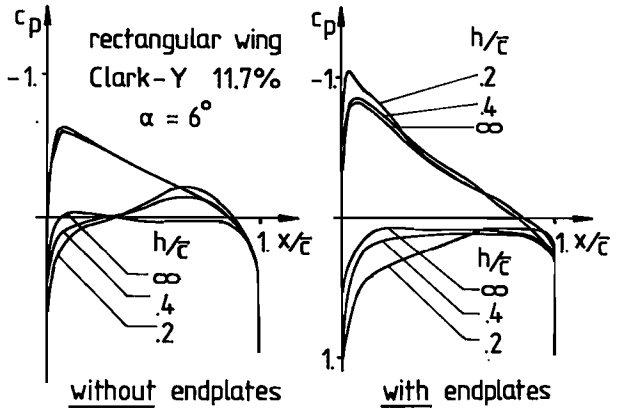

Fig. 4.5 Influence of endplates on pressure distribution at the outer wing section

Fig. 4.5 compares the pressure distribution for outer wing section with and without endplates. It will be noticed that endplates give a smaller unloading of the rear part of the tip section. But the loading of the foreward part of the section is remarkably increased in comparison to the wing without endplates. As a result of this the c.p. will be moving in the forward direction, if the wing approaches the ground. This means that the height stability is favourably influenced by endplates. The effect can be seen in Fig. 4.6 where F_m is compared for both types of wings.

It is remarkable and perhaps surprisingly, a modification of the flow pattern near the wing tip can have an essential influence on static height stability.

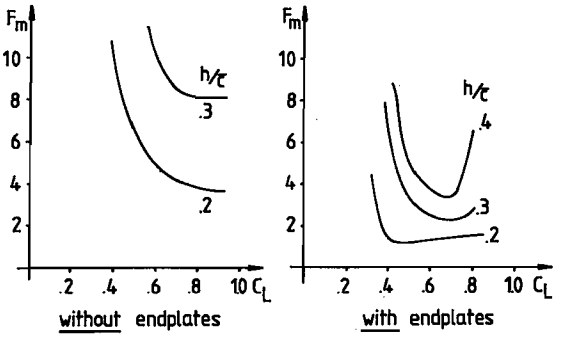

Fig. 4.6 Influence of endplates upon static height stability

This insight suggests a modification of the wing planform near the wing tip in such a way that the c.p. would be moved foreward near ground by a higher unloading of the rear part of the tip section. Fig. 4.7 presents the wing planform chosen. By sweeping back the outer part of the wing is nearly parallel to the lateral outflow. That gives a stronger suction force at the trailing edge of the swept parts of the wing leading to the desired movement of c.p. in the forward direction if the wing approaches the ground.

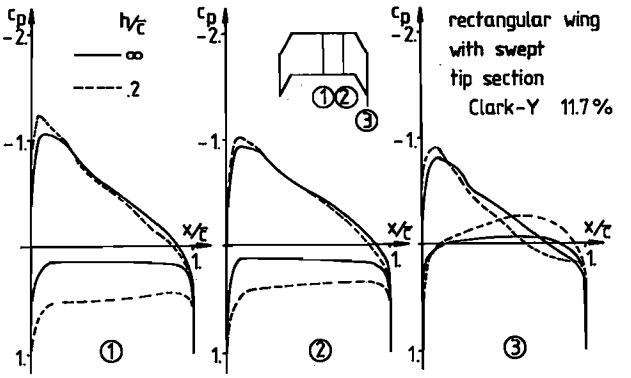

Fig. 4.7 Pressure distribution of a wing with swept tip sections

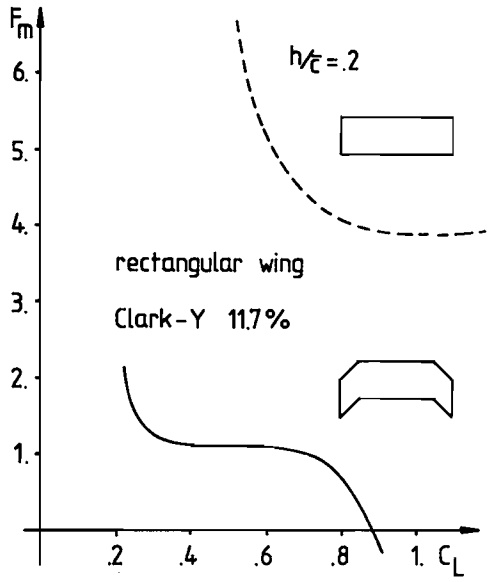

Fig. 4.8 Static height stability of a wing with swept tip sections

With this configuration we can even get the wing stable as shown in Fig. 4.8. The results of this section indicate, that a suitable combination of airfoil sections, wing planform and endplates or winglets could lead to satisfactory height stability without using a horizontal tail.

5. Ground effect during landings

It is evident from the deliberations in the previous sections that ground effect must influence the vertical motion even of conventional aircraft configurations during the final phase of landings. As mentioned in section 2, the ground effect reduces the large effective camber of high-lift wing configurations and leads to positive values of c_{Lh}, which makes the vertical motion in ground effect unstable. Fig. 5.1 shows the variation of lift coefficient and pitching moment coefficient with height and angle of attack for a typical high-lift configuration. Fig. 5.2 presents the corresponding curves for a ram-wing vehicle with height stability.

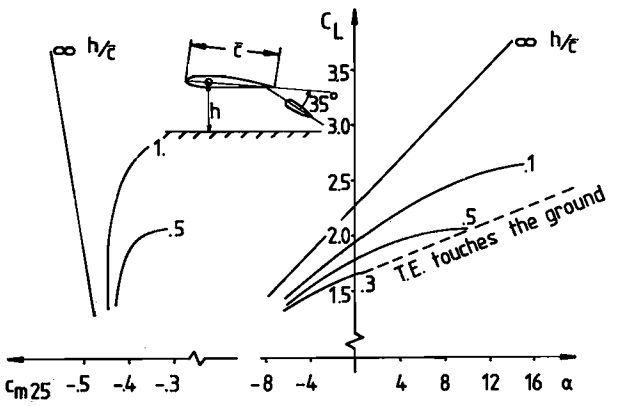

Fig. 5.1 Lift and pitching moment coefficients of a conventional high-lift configuration

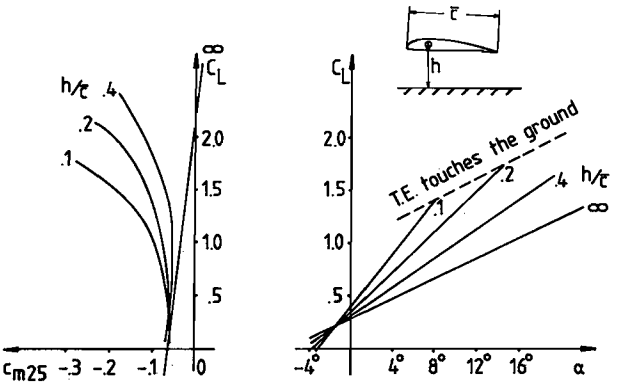

Fig. 5.2 Lift and pitching moment coefficients of a typical WIG configuration

The influence of ground effect can be best shown by a comparison of automatic flare maneuvers for both types of vehicles. The control law for this maneuver is given by

$$\Delta c_m = K_1(h-h_c) + K_2\dot{h} \tag{5.1}$$

where the coefficients, identical for both vehicles, have been optimized for a flare without

ground effect. Fig. 5.3 presents the results of a simulation of this maneuver, with and without ground effect, for the conventional aircraft, while Fig. 5.4 plots the corresponding functions for a flare of the ram-wing vehicle. From Fig. 5.3 it is seen that the work load of the control system is much higher for the conventional configuration than we found in Fig. 5.4. The closed-loop stability is, obviously, remarkable different for both types of vehicles as a consequence of the difference in static and dynamic height stability inherent to the configurations. It seems important to point out that the airspeed was held constant during the simulated flare maneuvers. Thus, the effect, revealed by the simulation, is not induced by a coupling between height and speed as is the case in phugoid motions. Only height and the rotational degree of freedom take part in the observed motion.

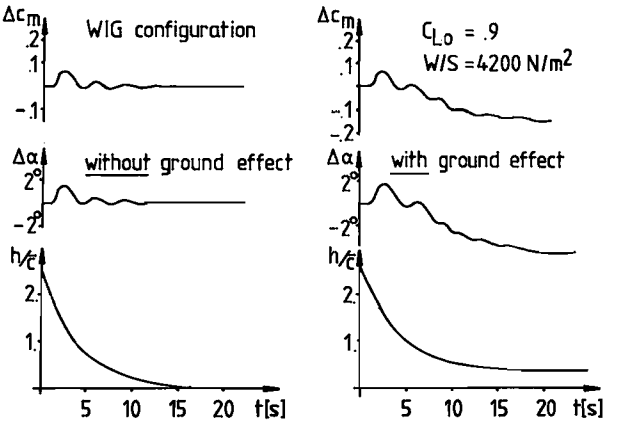

Fig. 5.4 Controled flare of a WIG configuration

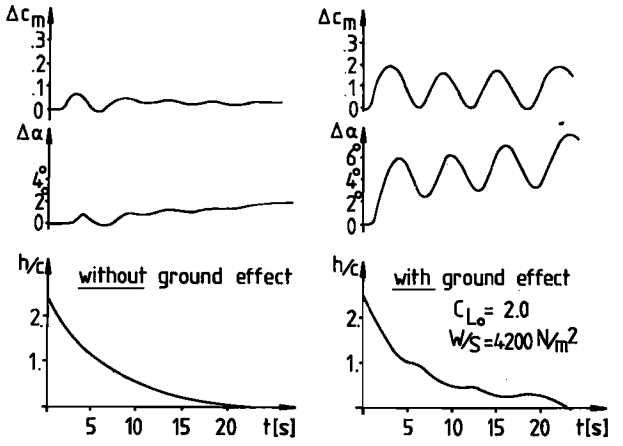

Fig. 5.3 Automatic flare of a conventional high-lift configuration

6. Conclusions

The paper is concerned with the strong interrelationship between aerodynamic configuration and longitudinal stability in ground effect. The following conclusions were made:

1. Longitudinal stability is an important factor affecting the design of wing-in-ground vehicles (WIGs).

2. Longitudinal motion in ground effect reveals modes and stability conditions remarkably different from o.g.e. relationships.

3. Approaching the ground the "phugoid mode" breaks into an aperiode mode and an oscillatory mode involving vertical and pitching motion. Stability in height is a firm requirement for WIGs.

4. Analyzing the fifth-order characteristic equation i.g.e. a new type of static stability,

called "static height stability", has been found. The corresponding stability condition can be expressed as a relationship between derivatives of the c.p. position with respect to height and angle of attack.

5. Static height stability requires a suitable aerodynamic configuration, it cannot be achieved by shifting the c.g..

6. The incorporation of horizontal tails, positioned out of ground, has a favourable effect on height stability.

7. In order to reduce the tail volume, new airfoil sections, characterized by a S-type mean line, have been developed. These airfoils are inherent stable over a large range of the lift coefficient.

8. Preliminary studies of wing configurations have shown the great effect of shaping the tip of a rectangular wing. Endplates and swept tip sections will improve height stability.

9. Conventional a/c, especially with flaps deflected, are basically static and dynamic unstable i.g.e.

10. Simulations, comparing flare maneuvers of a conventional and a WIG configuration, have revealed the different impact of ground effect on the time histories of longitudinal motion and elevator activity.

7. References

1. Wieselsberger, C., "Über den Flügelwiderstand in der Nähe des Bodens", Z. Flugtechn. Motorluftschiffahrt 12, 1921, pp. 145-147.

2. Lippisch, A. M., "Der 'Aerodynamische Bodeneffekt' und die Entwicklung des Flugflächen-(Aerofoil-)Bootes". Luftfahrttechnik-Raumfahrttechnik 10, 1964, pp. 261-269.

3. Ashill, P. R., "On the Minimum Induced Drag of Ground-Effect Wings". Aeronautical Quarterly, August 1970, pp. 211-231.

4. Gallington, R. W., Krause, F. H., "Recent Advances in Wing-in-Ground-Effect Vehicle Technologie". AIAA/SNAME Advanced Marine Vehicles Conference, Arlington, Va., Sept. 1976.

5. Staufenbiel, R. W., Yeh, B. T., "Flugeigenschaften in der Längsbewegung von Bodeneffekt-Fluggeräten, Teil I und II", ZFW 24, 1976, Jan./Febr., pp. 3-9, März/April, pp. 65-70.

6. Liebeck, R. H., "On the Design of Subsonic Airfoils for High Lift", AIAA Paper No. 76-406, 1976.

7. Steinbach, D., "Berechnung der Strömung mit Ablösung für Profile und Profilsysteme in Bodennähe oder in geschlossenen Kanälen". DFVLR-AVA IB 251-77 A02, 1977.

8. Stevens, W. A., Goradia, S. H., Braden, J. A., "Mathematical Model for Two-Dimensional Multi-Component Airfoils in Viscous Flow". NASA CR-1843, 1971.